

# A New Clustering Framework

BY HAO CHEN AND XIANCHENG LIN

*Department of Statistics, University of California, Davis,  
One Shields Avenue, Davis, California, 95616, U.S.A.*

hxchen@ucdavis.edu xclin@ucdavis.edu

## SUMMARY

Detecting clusters is a critical task in various fields, including statistics, engineering and bioinformatics. Our focus is primarily on the modern high-dimensional scenario, where traditional methods often fail due to the curse of dimensionality. In this study, we introduce a non-parametric framework for clustering that is applicable to any number of dimensions. Simulation results demonstrate that this new framework surpasses existing methods across a wide range of settings. We illustrate the proposed method with real data applications in distinguishing cancer tissues from normal tissues through gene expression data.

*Some key words:* Curse of dimensionality, Multivariate analysis, High-dimensional data, Gaussian mixture, Gene microarray.

## 1. INTRODUCTION

Cluster analysis, or clustering, is a fundamental problem in statistics. Broadly speaking, the task is to group a set of objects into clusters in such a way that the objects in one cluster are more “similar” to each other than to those in other clusters. The definition for “similar” can be somewhat arbitrary. In the following, we discuss this through a few toy examples and establish the criterion we will use for the paper.

### 1.1. What is “similar”?

Here are some toy examples in two dimensions. Figure 1 shows the data colored according to their generating schemes. We applied two classical clustering algorithms to these data: the

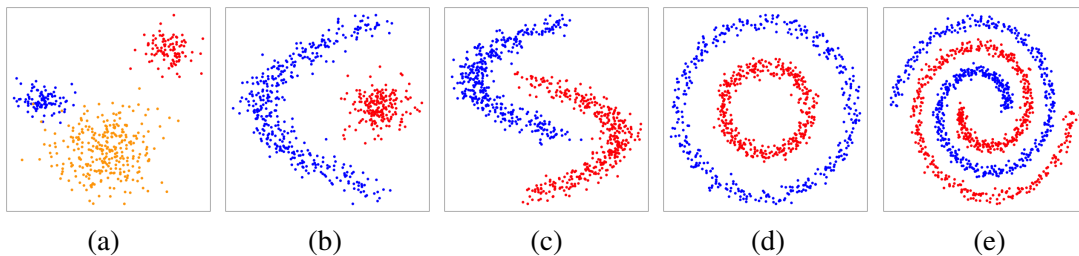


Fig. 1: Examples of different shapes of two-dimensional data, with different colors representing different data generating schemes: (a) three samples generated from three bivariate Gaussian distributions; (b) one sample from a bivariate Gaussian distribution and another from a parabola with perturbations; (c) two parabolas with perturbations; (d) two rings with perturbations; and (e) two logarithmic spirals with perturbations.

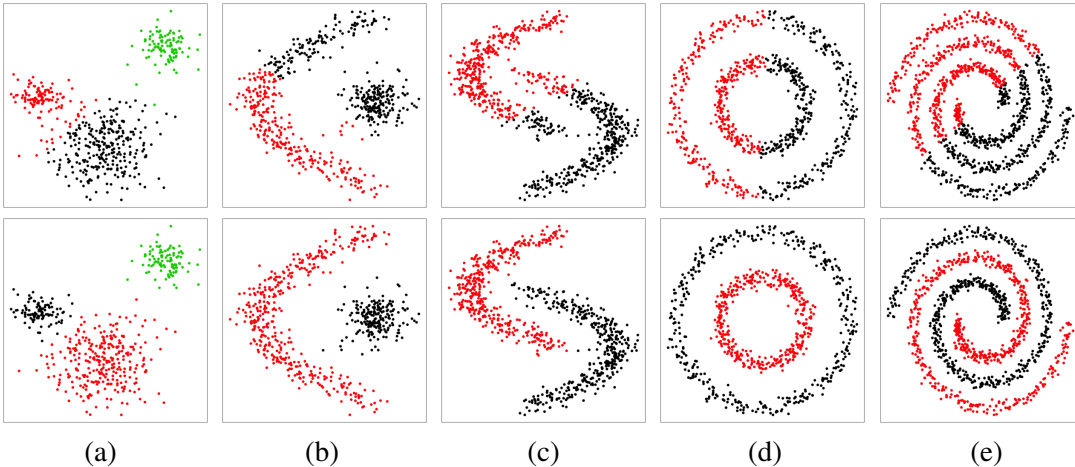


Fig. 2: Clustering results based on the standard  $k$ -means approach (top row) and the spectral clustering (bottom row) for the five datasets in Figure 1.

standard  $k$ -means clustering algorithm (`kmeans` function in R) and spectral clustering (`specc` function in the R package `kernlab`). The clustering results are shown in Figure 2.

The clustering results based on spectral clustering are much more satisfying. Hence, even though the definition of “similar” can be somewhat arbitrary, one likely wants to separate observations from different data generating schemes into distinct clusters. Generally speaking, cluster analysis is useful when the dataset consists of a mixture of observations from different underlying data-generating schemes or models, and we aim to *partition the observations into clusters such that each cluster can be modeled simply*, for instance, using a function or distribution. This allows us to summarize the dataset concisely and implement different treatments for different clusters according to their properties. In the examples above, the  $k$ -means approach minimizes the within-cluster sum of squares (group ‘similar’ points to some extent); however, it does not facilitate the follow-up task of understanding the observations in each cluster, making it less useful.

In the following, we refer to points that can be represented by a relatively simple distribution or model as one cluster, and our goal is to group observations that are *similar in underlying distribution or model*.

### 1.2. Difficulties in clustering high-dimensional data

In Section 1.1, spectral clustering performs well across all examples. However, this may not be the case when the dimensionality of the data is high. Consider a scenario where the data is a mixture of observations from two distributions,  $\mathcal{N}_d(\mathbf{0}, \Sigma)$  and  $\mathcal{N}_d(a\mathbf{1}, b\Sigma)$ , with  $d = 800$  and  $\Sigma_{ij} = 0.1^{|i-j|}$ , where  $\Sigma_{ij}$  is the  $(i, j)$ th element of  $\Sigma$ . Suppose there are 50 observations in each cluster, and the goal is to separate them. We examine two simulation settings:

- Setting 1 (only mean differs):  $a = 0.25$ ,  $b = 1$ .
- Setting 2 (only variance differs):  $a = 0$ ,  $b = 1.2$ .

For spectral clustering, we use an advanced choice, `kpar = ‘local’`, in the `specc` function to avoid unexpected errors encountered with high-dimensional data (details in Supplement S1). Spectral clustering encompasses various methods, each differing in their approach to constructing similarity graphs and handling data complexity. Therefore, in addition to `specc`, we include the method described in Chapter 14.5.3 of [Hastie et al. \(2009\)](#) (Spectral), which involves constructing

Table 1: Mis-clustering rates for various clustering methods under two settings. The smallest mis-clustering rate under each setting is in bold.

	Spectral	Specc	RSpec(A)	RSpec(L)	IF-PCA	<i>t</i> -SNE
Setting 1	0.157	<b>0.006</b>	0.279	0.167	0.254	0.098
Setting 2	0.467	0.446	0.418	<b>0.371</b>	0.451	0.462

a 10-NN similarity graph and applying conventional spectral clustering. We also include the Regularized Spectral Clustering method proposed by [Rohe et al. \(2011\)](#) (`reg.SP` in the R package `randnet`) to the same similarity graph for both the adjacency matrix (RSpecA) and laplacian matrix (RSpecL). Additionally, we apply some recently popular clustering methods. IF-PCA, proposed by [Jin & Wang \(2016\)](#), has shown successes in clustering gene microarray data. *t*-SNE (*t*-distributed stochastic neighbor embedding) ([Maaten & Hinton, 2008](#)) was initially proposed for data visualization by projecting observations into a two-dimensional space, effectively groups “similar” observations in this space. [Mwangi et al. \(2014\)](#) proposed to use the *k*-means clustering algorithm on the two-dimensional projected data from *t*-SNE. We apply these methods to the data generated from the two settings above, and the mis-clustering rates from a typical simulation run are shown in Table 1.

Setting 1 is a relatively straightforward case where the two clusters differ only in mean. In this scenario, we see that `specc` achieves the best performance. Setting 2 is more complex, with the two clusters differing in scale. All methods struggle in this setting. For spectral clustering, it is closely related to the Mincut problem when observations are represented through a similarity graph. When the dimension is high and the two clusters differ in scale, the curse of dimensionality causes the observations in the cluster with larger variance to be more sparsely scattered than those in the cluster with smaller variance. As a result, for any observation in the cluster with larger variance, its nearest points tend to be from the other cluster, causing the spectral clustering to fail. We explore this phenomenon further in Section 2.

In this paper, we propose a new clustering criterion based on theoretical results (Section 2). The new method is compared with existing methods under various settings in Section 3 and applied to real data applications in Section 4. The paper concludes with discussions in Section 5.

## 2. PROPOSED METHOD

### 2.1. Graph partition methods review

First, we review the graph clustering problem since our method will be based on similarity graphs constructed from the observations. The primary graph clustering formulations focus on graph cut and partitioning problems ([Chan et al., 1993](#); [Shi & Malik, 2000](#)). MinCut is an example of a traditional graph partitioning method. The MinCut method focuses on identifying the partition of a graph into two disjoint sets by minimizing the number of cut edges. The objective is to separate the graph into clusters with the fewest possible inter-cluster connections. However, [Wu & Leahy \(1993\)](#) observed that in many tested graphs, the solutions of this problem are partitions with isolated nodes in clusters. The Ratio Cut method ([Leighton & Rao, 1988](#)) improves upon MinCut by considering the number of nodes in each clusters, avoiding isolated nodes. Later, the Normalized Cut (Ncut) method ([Shi & Malik, 2000](#)) seeks to minimize the cut relative to the number of edges in a cluster instead of the number of nodes. It has been shown that relaxing Ncut leads to normalized spectral clustering, while relaxing RatioCut results in unnormalized

spectral clustering on the graph laplacian matrix (Von Luxburg, 2007). Spectral clustering has since become more popular. However, when we investigate the similarity graphs constructed on the observations and take into account the patterns caused by the curse of dimensionality, some powerful statistics can be derived.

## 2.2. Notations

We use  $G_k$  to denote the set of edges in the  $k$ -nearest neighbor ( $k$ -NN) graph, and  $(i, j) \in G_k$  if node  $i$  points to node  $j$  (each node points to its first  $k$  nearest neighbors). Let  $x$  be an  $N$ -length vector of 1's and 2's, and define

$$R_{1,k}(x) = \sum_{(i,j) \in G_k} I_{x_i=x_j=1}, \quad R_{2,k}(x) = \sum_{(i,j) \in G_k} I_{x_i=x_j=2}.$$

Then,  $x$  divides the observations into two clusters: 1's (Cluster 1) and 2's (Cluster 2). Let  $m$  be the number of 1's in  $x$  and  $n$  be the number of 2's in  $x$ . We define  $p_{11,k}(x)$  as one  $k$ th of the probability that an observation in cluster 1 finds another observation in cluster 1 among its first  $k$  nearest neighbors, i.e.,  $p_{11,k}(x) = R_{1,k}(x)/(km)$ . Similarly, we have  $p_{12,k}(x) = (km_x - R_{1,k}(x))/(km)$ ,  $p_{21,k}(x) = R_{2,k}(x)/(kn)$ ,  $p_{22,k}(x) = (kn - R_{2,k}(x))/(kn)$ . It is clear that

$$p_{11,k}(x) + p_{12,k}(x) = 1, \quad p_{21,k}(x) + p_{22,k}(x) = 1.$$

Let  $x^*$  represent the true clustering, with  $m^*$  1's and  $n^*$  2's in  $x^*$  ( $m^* + n^* = N$ ). We define  $p_{11}^{(0)}$  and  $p_{22}^{(0)}$  as the expected values of  $p_{11,k}$  and  $p_{22,k}$  when the two clusters are from the same distribution:

$$p_{11}^{(0)} = \frac{m^*-1}{N-1}, \quad p_{22}^{(0)} = \frac{n^*-1}{N-1}.$$

## 2.3. Patterns in high dimensions

We explore how the curse of dimensionality manifests. Figure 3 plots the average probabilities of observations in sample 1 and sample 2 finding  $k$  nearest neighbors within the sample. If a  $k$ -NN graph on the pooled observations is constructed such that each observation points to its first  $k$  nearest neighbors, then  $p_{11}$  is defined as the number of edges in the graph pointing from an observation in sample 1 to another in sample 1 divided by the total number of edges pointing from an observation in sample 1. Similarly,  $p_{22}$  is defined for sample 2. Here, sample 1 contains  $m$  observations randomly generated from  $\mathcal{N}_d(\mathbf{0}, \Sigma)$ , and sample 2 contains  $n$  observations randomly generated from  $\mathcal{N}_d(a\mathbf{1}, b\Sigma)$ , where  $d = 200$  and  $\Sigma_{ij} = 0.1^{|i-j|}$ . We consider three settings:

- Setting 0 (same distribution):  $a = 0, b = 1$ .
- Setting 1 (mean differs):  $a = 0.3, b = 1$ .
- Setting 2 (mean and variance differ):  $a = 0.3, b = 1.3$ .

When the two samples are from the same distribution, the probability that one observation finds another observation among its first  $k$  nearest neighbors is always  $k/(N-1)$ . Let  $p_{11}^{(0)}$  and  $p_{22}^{(0)}$  be the expectations of  $p_{11}$  and  $p_{22}$  when the two samples are from the same distribution. Then  $p_{11}^{(0)} = (m-1)/(N-1)$  and  $p_{22}^{(0)} = (n-1)/(N-1)$ . Under setting 0, we see that  $p_{11}$  and  $p_{22}$  are close to  $p_{11}^{(0)}$  and  $p_{22}^{(0)}$ , respectively, across all  $k$  values.

When the two samples are from different distributions with a mean difference,  $p_{11}$  and  $p_{22}$  are larger than  $p_{11}^{(0)}$  and  $p_{22}^{(0)}$ , respectively, until  $k = N-1$ , where each observation finds every other observations as its first  $N-1$  nearest neighbors.

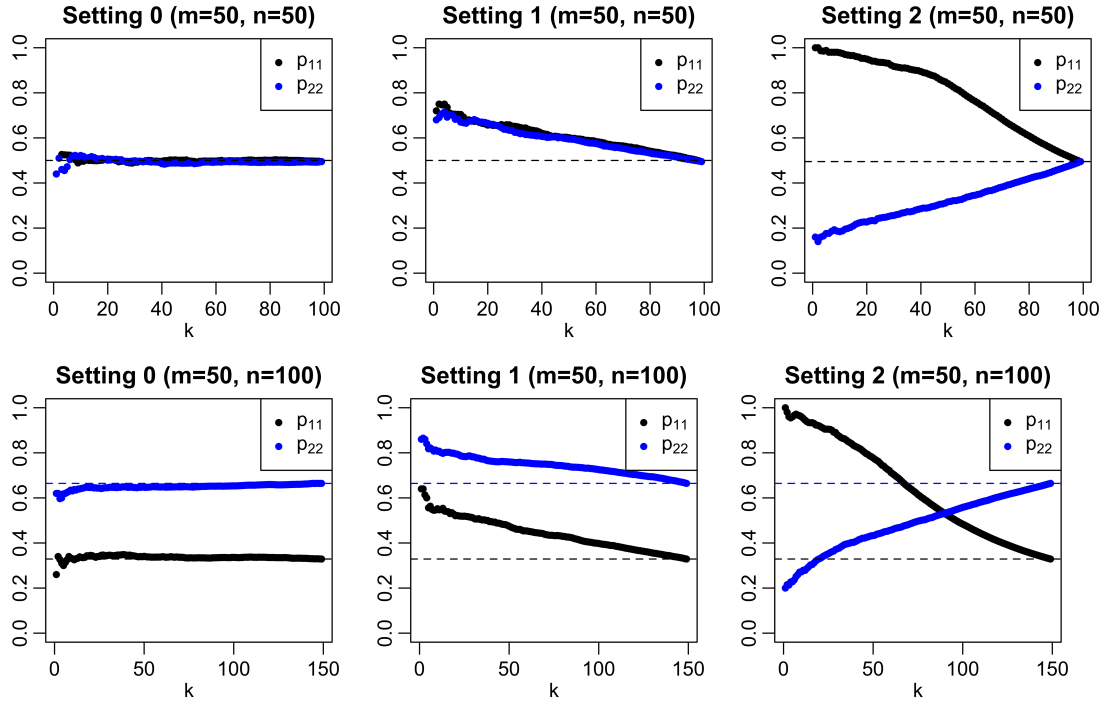


Fig. 3: Plots of  $p_{11}$  (black) and  $p_{22}$  (blue) considering  $k$  nearest neighbors under different settings. The dashed lines represent the baseline when the two clusters are from the same distribution  $p_{11}^{(0)} = (m-1)/(N-1)$  (black dashed line) and  $p_{22}^{(0)} = (n-1)/(N-1)$  (blue dashed line). The two dashed lines overlap when  $m = n$ .

When the two distributions differ in scale,  $p_{11}$  is larger than  $p_{11}^{(0)}$ , but  $p_{22}$  is smaller than  $p_{22}^{(0)}$  across all  $k$  values. This illustrates the curse of dimensionality. Here,  $d = 200$  and sample 2 is from a distribution with a larger variance than sample 1. As the volume of the space grows exponentially with dimension, observations in sample 2 tend to find observations in sample 1 to be closer than other observations in sample 2, resulting in  $p_{22}$  being smaller than  $p_{22}^{(0)}$ .

#### 2.4. New clustering criteria

If the two clusters are indeed from two different distributions, we would have the following three possible scenarios for some  $k$ 's according to Section 2.3:

- (1)  $p_{11,k}(x^*) > p_{11}^{(0)}, p_{22,k}(x^*) > p_{22}^{(0)}$ ,
- (2)  $p_{11,k}(x^*) > p_{11}^{(0)}, p_{22,k}(x^*) < p_{22}^{(0)}$ ,
- (3)  $p_{11,k}(x^*) < p_{11}^{(0)}, p_{22,k}(x^*) > p_{22}^{(0)}$ .

From Figure 3, we see that  $p_{11,k}(x^*)$  and  $p_{22,k}(x^*)$  depend on  $k$ . Here, we first fix  $k$  and discuss the clustering criteria with the aim of finding  $x^*$ . We will then discuss the choice of  $k$  in Section 2.5. For notation simplicity, we use  $R_1(x)$  and  $R_2(x)$  instead of  $R_{1,k}(x)$  and  $R_{2,k}(x)$  in the rest of this section.

We borrow strengths from graph-based two-sample tests (Chen & Friedman, 2017) and propose to use the following two quantities:

$$\begin{aligned} Z_w(x) &= \frac{R_w(x) - \mu_w(x)}{\sigma_w(x)}, & R_w(x) &= \frac{n-1}{N-2}R_1(x) + \frac{m-1}{N-2}R_2(x), \\ Z_d(x) &= \frac{R_d(x) - \mu_d(x)}{\sigma_d(x)}, & R_d(x) &= R_1(x) - R_2(x), \end{aligned}$$

where  $\mu_w(x)$ ,  $\sigma_w(x)$ ,  $\mu_d(x)$ ,  $\sigma_d(x)$  are normalizing terms so that  $Z_w(x)$  and  $Z_d(x)$  are properly standardized to have mean 0 and variance 1 if there is only one cluster. Their expressions can be obtained through similar treatments under the two-sample testing setting (Schilling, 1986; Henze, 1988) and the change-point detection setting (Liu & Chen, 2022). Let  $\mathcal{X}_m$  be the set of all  $x$ 's with  $m$  1's and  $(N - m) = n$  0's. Then, for  $x \in \mathcal{X}_m$ , we have,

$$\begin{aligned} \mu_w(x) &= \frac{(m-1)(n-1)}{(N-1)(N-2)}kN, \\ \sigma_w(x) &= \frac{mn(m-1)(n-1)}{N(N-1)(N-2)(N-3)} \left( kN + q_{1,k} - \frac{1}{N-2}(q_{2,k} + kN - k^2N) - \frac{2}{N-1}k^2N \right), \\ \mu_d(x) &= k(m - n), \\ \sigma_d(x) &= \frac{mn}{N(N-1)}(q_{2,k} + kN - k^2N). \end{aligned}$$

where  $q_{1,k} = \sum_{(i,j) \in G_k} I_{(j,i) \in G_k}$  and  $q_{2,k} = \sum_{i=1}^N \sum_{j \neq i} I_{(j,i), (i,j) \in G_k}$ .

Define  $E_2(\cdot)$  as the expectation under the assumption that there are two clusters.

**THEOREM 1.** *For any fixed  $k$ , if  $p_{11,k}(x^*)$  and  $p_{22,k}(x^*)$  fall into any of the three scenarios, we have:*

- Under scenario (1),  $E_2(Z_w(x))$  is maximized at  $x = x^*$  or  $x = 1 - x^*$ .
- Under scenario (2),  $E_2(Z_d(x))$  is maximized at  $x = x^*$ .
- Under scenario (3),  $E_2(Z_d(x))$  is maximized at  $x = 1 - x^*$ .

Based on the above theorem, we could use  $\max_x Z_w(x)$  to cluster in scenario (1), and use  $\max_x Z_d(x)$  to cluster in scenarios (2) and (3). However, in practice, we won't know which scenario it is, so we propose to use

$$M_\kappa(x) = \max(Z_w(x), \kappa Z_d(x))$$

as the criterion. The choice of  $\kappa$  is discussed in Section 2.6 with  $\kappa = 1.55$  as the default choice. Table 2 adds the mis-clustering rate of the new method to Table 1. We see that the mis-clustering rate of the new method under setting 1 is on par with the best remaining methods, and the mis-clustering rate of the new method under setting 2 is much lower than all other methods.

Table 2: Mis-clustering rate under the same settings as in Table 1.

	Spectral	Specc	RSpec(A)	RSpec(L)	IF-PCA	$t$ -SNE	New
Setting 1	0.157	<b>0.006</b>	0.279	0.167	0.254	0.098	0.010
Setting 2	0.467	0.446	0.418	0.371	0.451	0.462	<b>0.041</b>

*Remark 1.* It can also be shown that, under scenario (1),  $E_2(R_w(x)) - \mu_w(x)$  is maximized at  $x = x^*$  or  $x = 1 - x^*$ ; under scenario (2),  $E_2(R_d(x)) - \mu_d(x)$  is maximized at  $x = x^*$ ; under scenario (3),  $E_2(R_d(x)) - \mu_d(x)$  is maximized at  $x = 1 - x^*$ . However, we do not recommend using  $R_w(x) - \mu_w(x)$  and  $R_d(x) - \mu_d(x)$  as the criteria because they are not well normalized and are difficult to combine if one does not know which scenario the actual data falls in.

*Proof.* We first compute  $E_2(R_w(x))$  and  $E_2(R_d(x))$ . For  $x$ , suppose there are  $\Delta_1 \in [0, m^*]$  observations in cluster 1 placed into cluster 2, and  $\Delta_2 \in [0, n^*]$  observations in cluster 2 placed into cluster 1. So  $x \in \mathcal{X}_m$  with  $m = m^* - \Delta_1 + \Delta_2$ . Since  $k$  is fixed here, for simplicity, we denote  $p_{11,k}(x^*)$ ,  $p_{12,k}(x^*)$ ,  $p_{21,k}(x^*)$ ,  $p_{22,k}(x^*)$  by  $p_{11}^*$ ,  $p_{12}^*$ ,  $p_{21}^*$ ,  $p_{22}^*$ , respectively. Then, we have,

$$\begin{aligned} E_2(R_1(x)) &= p_{11}^* k m^* \frac{(m^* - \Delta_1)(m^* - \Delta_1 - 1)}{m^*(m^* - 1)} + p_{12}^* k m^* \frac{(m^* - \Delta_1)\Delta_2}{m^* n^*} + p_{21}^* k n^* \frac{(m^* - \Delta_1)\Delta_2}{m^* n^*} + p_{22}^* k n^* \frac{\Delta_2(\Delta_2 - 1)}{n^*(n^* - 1)}, \\ E_2(R_2(x)) &= p_{22}^* k n^* \frac{(n^* - \Delta_2)(n^* - \Delta_2 - 1)}{n^*(n^* - 1)} + p_{21}^* k n^* \frac{(n^* - \Delta_2)\Delta_1}{n^* m^*} + p_{12}^* k m^* \frac{(n^* - \Delta_2)\Delta_1}{n^* m^*} + p_{11}^* k m^* \frac{\Delta_1(\Delta_1 - 1)}{m^*(m^* - 1)}, \\ E_2(R_w(x)) &= \frac{n^* + \Delta_1 - \Delta_2 - 1}{N - 2} E_2(R_1(x)) + \frac{m^* - \Delta_1 + \Delta_2 - 1}{N - 2} E_2(R_2(x)) \\ &= k \frac{m^*(n^* - 1)p_{11}^* + n^*(m^* - 1)p_{22}^*}{N - 2} + k \frac{m^*(n^* - 1)p_{11}^* + n^*(m^* - 1)p_{22}^* - N(m^* - 1)}{m^*(m^* - 1)(N - 2)} \Delta_1^2 \\ &\quad + k \frac{m^*(n^* - 1)p_{11}^* + n^*(m^* - 1)p_{22}^* - N(n^* - 1)}{n^*(n^* - 1)(N - 2)} \Delta_2^2 + 2k \frac{m^*(n^* - 1)p_{11}^* + n^*(m^* - 1)p_{22}^* + N}{m^* n^*(N - 2)} \Delta_1 \Delta_2 \\ &\quad - k \Delta_1 \frac{(2m^* - 1)(m^*(n^* - 1)p_{11}^* + n^*(m^* - 1)p_{22}^*) - N(m^* - 1)^2}{m^*(m^* - 1)(N - 2)} \\ &\quad - k \Delta_2 \frac{(2n^* - 1)(m^*(n^* - 1)p_{11}^* + n^*(m^* - 1)p_{22}^*) - N(n^* - 1)^2}{n^*(n^* - 1)(N - 2)}, \\ E_2(R_d(x)) &= E_2(R_1(x)) - E_2(R_2(x)) \\ &= p_{11}^* k m^* - p_{22}^* k n^* - k \Delta_1 \left( p_{11}^* - \frac{n^*}{m^*} p_{22}^* + \frac{N}{m^*} \right) + k \Delta_2 \left( p_{22}^* - \frac{m^*}{n^*} p_{11}^* + \frac{N}{n^*} \right). \end{aligned}$$

We start with  $E_2(Z_d(x))$  as it is relatively simpler, and some of the intermediate results can be used for  $E_2(Z_w(x))$ . Notice that

$$\begin{aligned} E_2(R_d(x)) - \mu_d(x) &= p_{11}^* k m^* - p_{22}^* k n^* - k(m - n) - k \Delta_1 \left( p_{11}^* - \frac{n^*}{m^*} p_{22}^* + \frac{N}{m^*} \right) + k \Delta_2 \left( p_{22}^* - \frac{m^*}{n^*} p_{11}^* + \frac{N}{n^*} \right) \\ &= k(p_{11}^* m^* - p_{22}^* n^* - (m^* - n^*)) - k \Delta_1 \left( p_{11}^* - \frac{n^*}{m^*} p_{22}^* + \frac{N}{m^*} - 2 \right) + k \Delta_2 \left( p_{22}^* - \frac{m^*}{n^*} p_{11}^* + \frac{N}{n^*} - 2 \right) \\ &= (p_{11}^* m^* - p_{22}^* n^* - (m^* - n^*)) k \left( 1 - \frac{\Delta_1}{m^*} - \frac{\Delta_2}{n^*} \right). \end{aligned}$$

Then

$$E_2(Z_d(x)) = \frac{E_2(R_d(x)) - \mu_d(x)}{\sigma_d(x)} = (p_{11}^* m^* - p_{22}^* n^* - (m^* - n^*)) k f_d(\Delta_1, \Delta_2),$$

where

$$f_d(\Delta_1, \Delta_2) = \frac{1 - \frac{\Delta_1}{m^*} - \frac{\Delta_2}{n^*}}{\sqrt{(m^* - \Delta_1 + \Delta_2)(n^* + \Delta_1 - \Delta_2)}}.$$

Note that

$$\frac{\partial f_d}{\partial \Delta_1} = -\frac{N}{2m^* n^*} \frac{(n^* - \Delta_2)(m^* - \Delta_1 + 2\Delta_2) + \Delta_1 \Delta_2}{(m^* - \Delta_1 + \Delta_2)^{1.5} (n^* + \Delta_1 - \Delta_2)^{1.5}} < 0,$$

$$\frac{\partial f_d}{\partial \Delta_2} = -\frac{N}{2m^* n^*} \frac{(m^* - \Delta_1)(n^* - \Delta_2 + 2\Delta_1) + \Delta_1 \Delta_2}{(m^* - \Delta_1 + \Delta_2)^{1.5} (n^* + \Delta_1 - \Delta_2)^{1.5}} < 0.$$

So  $f_d(\Delta_1, \Delta_2)$  achieves its maximum when  $\Delta_1 = \Delta_2 = 0$  with the maximum being  $\frac{1}{\sqrt{m^* n^*}}$ , and achieve its minimum when  $\Delta_1 = m^*$ ,  $\Delta_2 = n^*$  with the minimum being  $-\frac{1}{\sqrt{m^* n^*}}$ . Also note that, under scenario (2), we have

$$p_{11}^* m^* - p_{22}^* n^* - (m^* - n^*) > \frac{m^* - 1}{N - 1} m^* - \frac{n^* - 1}{N - 1} - (m^* - n^*) = 0,$$

and under scenario (3), we have

$$p_{11}^* m^* - p_{22}^* n^* - (m^* - n^*) < 0.$$

Therefore, under scenario (2),  $E_2(Z_d(x))$  is maximized when  $\Delta_1 = \Delta_2 = 0$ , i.e., at  $x = x^*$ ; and under scenario (3),  $E_2(Z_d(x))$  is maximized when  $\Delta_1 = m^*$ ,  $\Delta_2 = n^*$ , i.e., at  $x = 1 - x^*$ .

Now, we move onto  $E_2(Z_w(x))$ . We first compute  $E_2(R_w(x)) - \mu_w(x)$ :

$$\begin{aligned} E_2(R_w(x)) - \mu_w(x) &= k \frac{m^*(n^*-1)p_{11}^* + n^*(m^*-1)p_{22}^* - \frac{(m^*-1)(n^*-1)N}{N-1}}{N-2} + k \frac{m^*(n^*-1)p_{11}^* + n^*(m^*-1)p_{22}^* - \frac{(m^*-1)(n^*-1)N}{N-1}}{m^*(m^*-1)(N-2)} \Delta_1^2 \\ &\quad + k \frac{m^*(n^*-1)p_{11}^* + n^*(m^*-1)p_{22}^* - \frac{(m^*-1)(n^*-1)N}{N-1}}{n^*(n^*-1)(N-2)} \Delta_2^2 + 2k \frac{m^*(n^*-1)p_{11}^* + n^*(m^*-1)p_{22}^* - \frac{(m^*-1)(n^*-1)N}{N-1}}{m^*n^*(N-2)} \Delta_1 \Delta_2 \\ &\quad - k \Delta_1 \frac{(2m^*-1)(m^*(n^*-1)p_{11}^* + n^*(m^*-1)p_{22}^* - \frac{(m^*-1)(n^*-1)N}{N-1})}{m^*(m^*-1)(N-2)} \\ &\quad - k \Delta_2 \frac{(2n^*-1)(m^*(n^*-1)p_{11}^* + n^*(m^*-1)p_{22}^* - \frac{(m^*-1)(n^*-1)N}{N-1})}{n^*(n^*-1)(N-2)} \\ &= k \frac{m^*(n^*-1)p_{11}^* + n^*(m^*-1)p_{22}^* - \frac{(m^*-1)(n^*-1)N}{N-1}}{N-2} \\ &\quad \times \left( 1 + \frac{\Delta_1^2}{m^*(m^*-1)} + \frac{\Delta_2^2}{n^*(n^*-1)} + \frac{2\Delta_1\Delta_2}{m^*n^*} - \frac{(2m^*-1)\Delta_1}{m^*(m^*-1)} - \frac{(2n^*-1)\Delta_2}{n^*(n^*-1)} \right). \end{aligned}$$

Then

$$E_2(Z_w(x)) = k \frac{m^*(n^*-1)p_{11}^* + n^*(m^*-1)p_{22}^* - \frac{(m^*-1)(n^*-1)N}{N-1}}{N-2} f_w(\Delta_1, \Delta_2),$$

where

$$f_w(\Delta_1, \Delta_2) = \frac{1 + \frac{\Delta_1^2}{m^*(m^*-1)} + \frac{\Delta_2^2}{n^*(n^*-1)} + \frac{2\Delta_1\Delta_2}{m^*n^*} - \frac{(2m^*-1)\Delta_1}{m^*(m^*-1)} - \frac{(2n^*-1)\Delta_2}{n^*(n^*-1)}}{\sqrt{(m^* - \Delta_1 + \Delta_2)(n^* + \Delta_1 - \Delta_2)(m^* - \Delta_1 + \Delta_2 - 1)(n^* + \Delta_1 - \Delta_2 - 1)}}.$$

It's complicated to work on  $f_w$  directly. Here, we first consider

$$\tilde{f}_d(\Delta_1, \Delta_2) = \frac{1 - \frac{\Delta_1}{m^*-1} - \frac{\Delta_2}{n^*-1}}{\sqrt{(m^* - \Delta_1 + \Delta_2 - 1)(n^* + \Delta_1 - \Delta_2 - 1)}}.$$

With similar arguments as for  $f_d(\Delta_1, \Delta_2)$ , we know that, for  $\Delta_1 \in [0, m^* - 1]$ ,  $\Delta_2 \in [0, n^* - 1]$ ,  $\tilde{f}_d(\Delta_1, \Delta_2)$  achieves its maximum when  $\Delta_1 = \Delta_2 = 0$  with the maximum being  $\frac{1}{\sqrt{(m^*-1)(n^*-1)}}$ , and

achieve its minimum when  $\Delta_1 = m^* - 1$ ,  $\Delta_2 = n^* - 1$  with the minimum being  $-\frac{1}{\sqrt{(m^*-1)(n^*-1)}}$ .

For the three corner cases  $(\Delta_1 = m^* - 1, \Delta_2 = n^*)$ ,  $(\Delta_1 = m^*, \Delta_2 = n^* - 1)$ ,  $(\Delta_1 = m^*, \Delta_2 = n^*)$ , we discuss them slightly later.

Hence, for  $\Delta_1 \in [0, m^* - 1]$ ,  $\Delta_2 \in [0, n^* - 1]$ , we have  $f_d(\Delta_1, \Delta_2)\tilde{f}_d(\Delta_1, \Delta_2)$  achieves its maximum at  $\Delta_1 = \Delta_2 = 0$  and  $\Delta_1 = m^* - 1$ ,  $\Delta_2 = n^* - 1$  with the maximum  $\frac{1}{\sqrt{m^*n^*(m^*-1)(n^*-1)}}$ . Notice that

$$f_w(\Delta_1, \Delta_2) = f_d(\Delta_1, \Delta_2)\tilde{f}_d(\Delta_1, \Delta_2) - h(\Delta_1, \Delta_2),$$

where

$$h(\Delta_1, \Delta_2) = \frac{\frac{N-2}{m^*n^*(m^*-1)(n^*-1)}\Delta_1\Delta_2}{\sqrt{(m^* - \Delta_1 + \Delta_2)(n^* + \Delta_1 - \Delta_2)(m^* - \Delta_1 + \Delta_2 - 1)(n^* + \Delta_1 - \Delta_2 - 1)}}.$$

Here,  $h(\Delta_1, \Delta_2) > 0$  when  $\Delta_1\Delta_2 > 0$ , so  $f_w(0, 0) > f_w(m^* - 1, n^* - 1)$ . For the three left out corner cases, we have

- $f_w(m^*, n^*) = \frac{1}{\sqrt{n^* m^* (n^* - 1)(m^* - 1)}} = f_w(0, 0)$ .
- $f_w(m^*, n^* - 1) = \frac{1 - \frac{2}{n^*}}{\sqrt{(n^* - 1)(m^* + 1)(n^* - 2)m^*}} = \frac{\sqrt{(1 - \frac{2}{n^*})(1 - \frac{2}{m^* + 1})}}{\sqrt{n^* m^* (n^* - 1)(m^* - 1)}} < f_w(0, 0)$ .
- $f_w(m^* - 1, n^*) = \frac{1 - \frac{2}{m^*}}{\sqrt{(n^* + 1)(m^* - 1)n^*(m^* - 2)}} = \frac{\sqrt{(1 - \frac{2}{m^*})(1 - \frac{2}{n^* + 1})}}{\sqrt{n^* m^* (n^* - 1)(m^* - 1)}} < f_w(0, 0)$ .  $\square$

Hence,  $f_w(\Delta_1, \Delta_2)$  achieves its maximum when  $\Delta_1 = \Delta_2 = 0$  or  $\Delta_1 = m^*, \Delta_2 = n^*$ . Under scenario (1),

$$\begin{aligned} & m^*(n^* - 1)p_{11}^* + n^*(m^* - 1)p_{22}^* - \frac{(m^* - 1)(n^* - 1)N}{N - 1} \\ & > m^*(n^* - 1)\frac{m^* - 1}{N - 1} + n^*(m^* - 1)\frac{n^* - 1}{N - 1} - \frac{(m^* - 1)(n^* - 1)N}{N - 1} = 0. \end{aligned}$$

So  $E_2(Z_d(x))$  achieves its maximum when  $\Delta_1 = \Delta_2 = 0$  or  $\Delta_1 = m^*, \Delta_2 = n^*$ , i.e., when  $x = x^*$  or  $x = 1 - x^*$ .

Given the results from Theorem 1, the next step is to find an efficient way to solve the optimization problem. Generally speaking, the optimization of  $Z_w(x)$  or  $Z_d(x)$  is an NP-hard problem. Instead of searching through the entire label assignment space, we address this task with a greedy algorithm. Suppose we are given an initial division vector  $\mathbf{x}$  of the clusters into two groups (this vector could be randomly generated). We then examine all possible single changes to  $\mathbf{x}$ , defined as changing one element in  $\mathbf{x}$  from  $s$  to  $1 - s$ , and choose the change that will result in the largest increase in the corresponding  $Z_w$  (or  $Z_d$ ). We continue making such moves until no further increase is possible. We start with many initial values for the partition  $\mathbf{x}$  and pick the result that yields the maximum value of  $Z_w$  (or  $Z_d$ ). Notice that at each step, we only change one element of  $\mathbf{x}$ . Therefore, it is unnecessary to loop over the entire adjacency matrix to calculate  $R_1, R_2, \sigma_d$ , and  $\sigma_w$  to update the values of  $Z_w(x)$  and  $Z_d(x)$ . Instead, we can only check the edges related to the label switch to calculate the increase or decrease in  $R_1$  and  $R_2$ . For  $\sigma_d$  and  $\sigma_w$ , the only terms related to the optimization process are  $m, n$ , which can be easily obtained in each step.

## 2.5. Choice of $k$

The first step of our clustering procedure is to construct  $G_k$  (the  $k$ -NN graph). Here,  $k$  can be any integer between 1 and  $N - 1$ . We can create all the possible  $G_k$  and perform the clustering process. Typically, different values of  $k$  lead to different clustering outcomes. Since the underlying true partition of the clusters is usually not available, a natural question arises: how to choose  $k$  such that the clustering criteria have the optimal power or give us the most reasonable partition. In this section, we intend to empirically discuss the choice of  $k$ .

We want to choose  $k$  such that  $p_{11,k}(x^*)$  and  $p_{22,k}(x^*)$  are far from  $p_{11}^{(0)}$  and  $p_{22}^{(0)}$ , while ensuring there are enough edges in the graph to contribute to the evidence. Heuristically, when the value of  $k$  is small, the graph is sparse and some useful similarity information among the individuals might not be fully captured by  $Z_w$  and  $Z_d$ . On the other hand, when  $k$  is too large, it includes some irrelevant information. If groundtruth is available for a given dataset, there always exists an optimal (or a few optimal) choice of  $k$  that will result in the partition with the largest overlap with the underlying true group assignments.

The choice of the hyper-parameter  $k$  under the two-sample testing and change-point detection regime for the statistic  $Z_w$  and  $Z_d$  was discussed in [Zhu & Chen \(2021\)](#), [Zhang & Chen \(2021\)](#) and [Zhou & Chen \(2022\)](#). Specifically, they consider the power of the methods for  $k = \lfloor N^\lambda \rfloor$  when

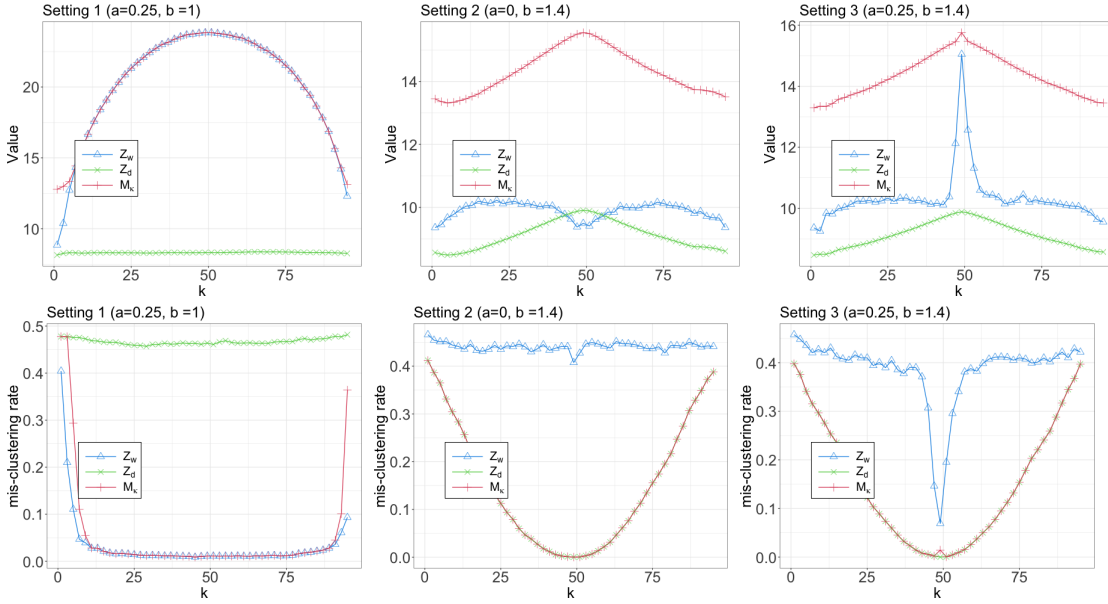


Fig. 4: Values of  $Z_w$ ,  $Z_d$ , and  $M_k$  (top panel) and mis-clustering rate (bottom panel) over  $k$ .  $m = n = 50$ .

varying  $\lambda$  from 0 to 1 in different settings. In two-sample testing, [Zhu & Chen \(2021\)](#) suggested using  $k = \lceil N^{0.5} \rceil$  with the  $k$ -MST, while [Zhou & Chen \(2022\)](#) suggested  $\lambda = 0.65$  for the  $k$ -NN graph.

Here, we explore the relation between  $k$  and mis-clustering rate. In particular, we aim to find out whether the  $k$  that leads to the maximum value of  $M_k$  results in the minimum clustering error. In each simulation setting, we generate the  $k$ -NN graphs for  $k$  from 1 to  $N - 3$ , increased by 2 at each time. We consider the Gaussian mixture example where we have two groups of samples from  $\mathcal{N}_d(\mathbf{0}, \Sigma)$  and  $\mathcal{N}_d(a\mathbf{1}, b\Sigma)$ , with  $\Sigma_{ij} = 0.1^{|i-j|}$ .

- Setting 1 (only mean differs):  $a > 0, b = 1$ .
- Setting 2 (only variance differs):  $a = 0, b > 1$ .
- Setting 3 (both mean and variance differ):  $a > 0, b > 1$ .

We first examine the values of  $Z_w$  and  $Z_d$  for different settings, along with the value of  $M_k$  with  $\kappa = 1.55$ , i.e.,  $M_k(x) = \max(Z_w(x), 1.55Z_d(x))$ . The choice of  $\kappa$  is discussed in Section 2.6. Here, our primary concern is the value of  $k$  that leads to the maximum  $M_k$ , and the value of  $\kappa$  does not affect this choice of  $k$  as long as  $\kappa$  is within a certain range. We set the dimension to be  $d = 800$ . For the cluster sizes, we examine both balanced ( $m = n = 50$ ) and unbalanced ( $m = 30, n = 70$ ) cases.

Figure 4 plots the values of  $Z_w$ ,  $Z_d$ , and  $M_k$  over  $k$  under all three settings for the balanced case (top panel), as well as the mis-clustering rate (bottom panel). We see that the mis-clustering rate reaches its minimum when  $M_k$  is at its maximum in all settings. The same pattern also appears for the unbalanced case (Figure 5). This is exciting, as  $M_k$  over  $k$  is fully observable given the data, allowing us to select the  $k$  that maximizes  $M_k$  in practice.

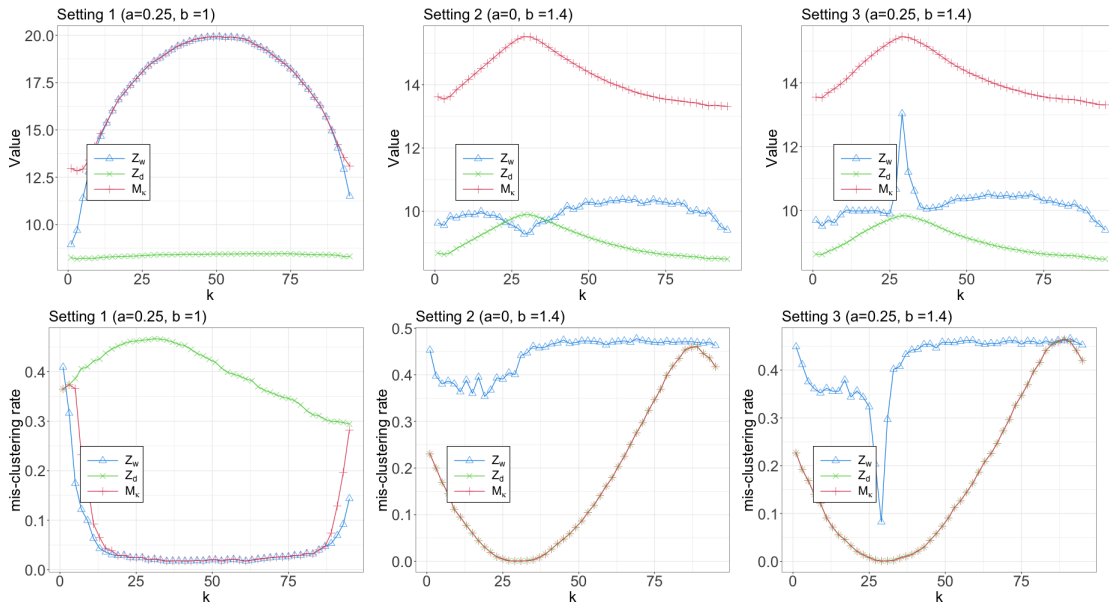


Fig. 5: Values of  $Z_w$ ,  $Z_d$ , and  $M_\kappa$  (top panel) and mis-clustering rate (bottom panel) over  $k$ .  $m = 30, n = 70$ .

## 2.6. Choice of $\kappa$

From Section 2.4,  $\max_x Z_w(x)$  can be used to cluster scenario (1), and  $\max_x Z_d(x)$  is suitable for scenarios (2) and (3). Since we don't know which scenario we are dealing with in reality,  $M_\kappa(x) = \max(Z_w(x), \kappa Z_d(x))$  was proposed for these three scenarios. Ideally, when the scenario is (1), we want  $Z_w$  to dominate in  $M_\kappa$ ; while when the scenario is (2) or (3), we want  $Z_d$  to dominate in  $M_\kappa$ . However, this dominance does not need to hold for all  $k$ 's. Instead, as long as  $M_\kappa$  picks the correct quantity ( $Z_w$  or  $Z_d$ ) when the correct quantity reaches its maximum, the goal is achieved given how we choose  $k$ . This can be seen clearly from Figure 4 and 5. In Figure 4 and 5, the leftmost pictures show two clusters generated from  $\mathcal{N}_d(\mathbf{0}, \Sigma)$  and  $\mathcal{N}_d(a\mathbf{1}, \Sigma)$ . This belongs to scenario (1), and  $Z_w$  should dominate  $M_\kappa$  based on the statements above. We see that  $M_\kappa$  is identical to  $Z_w$  when  $Z_w$  reach its maximum but differs from  $Z_w$  at the boundaries. That will not affect the mis-clustering rate using  $M_\kappa$  given how we choose  $k$ .

With these observations, we use the following simulation study to choose  $\kappa$ . All other parameters remain the same as in Figure 4 setting 1 (only mean differs). We gradually increase the location difference parameter  $a$  to determine the upper bound of  $\kappa$ . All other parameters remain the same as in Figure 4 setting 2 (only variance differs), we gradually increase the scale difference parameter  $b$  to determine the lower bound of  $\kappa$ . For each setting, we run 50 times.

In Figure 6, left panel, the mis-clustering rate significantly decreases at around  $a = 0.2$ . When the signal is less than this threshold, the difference between the two clusters is not substantial enough for the algorithm to distinguish them effectively, resulting in a mis-clustering rate close to 0.5. After this phase transition, the mis-clustering rate is much smaller. Therefore, we want  $Z_w$  to dominate in  $M_\kappa$  when  $a \geq 0.2$ , which means choosing  $\kappa$  smaller than the ratio when  $a \geq 0.2$ . This establishes an upper bound for  $\kappa$ , which is the minimum value of the boxplot at  $a = 0.2$ . Similarly, in the right panel, we want  $Z_d$  to dominate in  $M_\kappa$  when  $b \geq 1.15$ . This establishes a lower bound for  $\kappa$ , which is the maximum value of the boxplot at  $b = 1.15$ . Thus, a proper choice

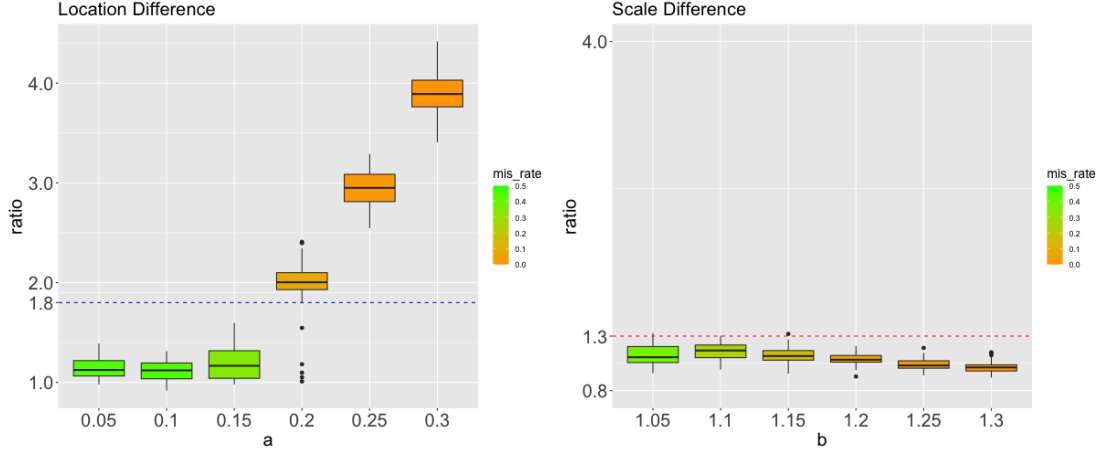


Fig. 6: Plots of ratio ( $r = Z_w/Z_d$ ) versus signal strength. Left panel: location difference with  $b = 1$ , and  $a$  increasing from 0.05 to 0.3. The blue dashed line at  $r = 1.8$  represents the minimum value of the boxplot when  $a = 0.2$ . The “mis\_rate” indicates the mean mis-clustering rate when using  $Z_w$  as the criterion, with green representing higher errors and orange indicating lower errors. Right panel: scale difference with  $a = 0$ , and  $b$  increasing from 1.05 to 1.3. The red dashed line at  $r = 1.3$  represents the maximum value of the boxplot when  $b = 1.15$ . The “mis\_rate” indicates the mean mis-clustering rate when using  $Z_d$  as the criterion, with green representing higher errors and orange indicating lower error.

of  $\kappa$  would be between the upper bound  $r = 1.8$  and the lower bound  $r = 1.3$ . For simplicity, we choose the middle point  $\kappa = 1.55$  as our default choice. It is important to note that if there is a prior probability indicating which of the three scenarios a particular problem belongs to, the choice of  $\kappa$  can be adjusted to favor more on  $Z_w$  or  $Z_d$  accordingly.

### 2.7. A ternary search algorithm

In this Section, we introduce a search algorithm for selecting  $k$  when computational resources are limited. Specifically, we focus on the algorithm of choosing  $k$  in Section 2.5. Notice that

$$\max_k M_\kappa = \max_k \max_x (Z_w(x), \kappa Z_d(x)).$$

To find the maximum value of  $M_\kappa$ , we need to determine the maximum values of  $Z_w$  and  $Z_d$  separately. From Theorem 1 and Figures 4 and 5, we observe that  $Z_d$  or  $Z_w$  is a unimodal function over  $k$  when it is the proper criterion. Therefore, we can use a ternary search algorithm to find the maximum value of  $M_\kappa$  (Bajwa et al., 2015). We summarize the algorithm below. For ease of notation, we denote the maximum value of  $Z_w(x)$  (or  $Z_d(x)$ ) on the  $k$ -NN graph  $G_k$  as  $f_k(x)$ . Based on Theorem 1, we note that for a given dataset, only one of  $Z_w$  or  $Z_d$  may be a unimodal function. While ternary search is guaranteed to find the optimal value for unimodal functions, it suffices for our purposes since the maximum value of  $M_\kappa$  corresponds to the maximum value of the unimodal function when it is the correct clustering criterion.

## 3. NUMERICAL STUDIES

In this section, we compare the performance of the new method with other existing methods on synthetic data. Specifically, we compare the following methods:

**Algorithm 1.** Ternary Search**Input:**  $f(k)$  for a series of  $k$ -NN graphs  $G_k$ .**Output:** The maximum value of  $f(k)$ .**Algorithm:**

1. Set `left` to 1 and `right` to  $N - 1$ .
2. While `right - left` is greater than 1, do the following:
  - a. Compute `left_third` as  $\lfloor \text{left} + (\text{right} - \text{left})/3 \rfloor$ .
  - b. Compute `right_third` as  $\lfloor \text{right} - (\text{right} - \text{left})/3 \rfloor$ .
  - c. If  $f(\text{left\_third})$  is less than  $f(\text{right\_third})$ , set `left` to `left_third`;
  - d. Otherwise, set `right` to `right_third`.
3. Return  $f\left(\left\lfloor \frac{\text{left} + \text{right}}{2} \right\rfloor\right)$ .

- Spectral: Spectral clustering as described in [Hastie et al. \(2009\)](#).
- Specc: The `specc` function in the `kernlab` package with `'kpar=local'`. (A discussion of the choice of “kpar” can be found in Supplement S1.)
- RSpecA and RSpecL: Regularized Spectral Clustering (`reg.SP` in the `randnet` package) proposed by [Rohe et al. \(2011\)](#), applied to the 10-NN adjacency matrix and the laplacian matrix, respectively.
- IF-PCA: Influential Feature PCA proposed by [Jin & Wang \(2016\)](#).
- $t$ -SNE: Using  $t$ -SNE to project the data into two dimensional space and then applying the  $k$ -means clustering algorithm on the projected data ([Mwangi et al., 2014](#)).

We consider a few different settings below:

- Gaussian mixture: Cluster 1:  $\mathbf{X}_1 \sim \mathcal{N}_d(\mathbf{0}, \Sigma)$  and Cluster 2:  $\mathbf{X}_2 \sim \mathcal{N}_d(a\mathbf{1}, b\Sigma)$ ,  $\Sigma_{ij} = 0.1^{|i-j|}$ . The location parameter  $a \in \{0, 0.1, 0.5\}$  and the scale parameter  $b \in \{0.8, 1, 1.4\}$ .
- $t$ -distribution mixture: Cluster 1:  $\mathbf{X}_1 \sim t_{20}(\mathbf{0}, \Sigma)$  and Cluster 2:  $\mathbf{X}_2 \sim t_{20}(a\mathbf{1}, b\Sigma)$ ,  $\Sigma_{ij} = 0.1^{|i-j|}$ . The location parameter  $a \in \{0, 0.25, 0.3\}$  and the scale parameter  $b \in \{0.8, 1, 3, 3.5\}$ .

For each setting, the mis-clustering rate is estimated through 50 simulation runs. Figure 7 is arranged in three columns representing location difference, scale difference, and location-scale difference, respectively. The first column displays the results for the traditional location difference Gaussian Mixture with a fixed covariance matrix. The top panel shows a small difference between clusters with  $a = 0.1$ , while the bottom panel shows a larger difference with  $a = 0.5$ . The second column displays the results for scale-only difference, considering both the variance parameter  $b > 1$  and  $b < 1$ . The third column combines the parameters from the first and second columns. We observe that, except for the top left panel where all methods are inefficient due to the small signal, the new method performs well for all other settings, either being the best or among the best methods. In particular, under scale difference (middle panel), our method dramatically outperforms the others.

Figure 8 shows mis-clustering rates for different methods under the mixture of two multivariate  $t$ -distributions. In the multivariate  $t$ -distribution location-difference mixture scenario,  $t$ -SNE performs very well when the difference is small, which is expected given how  $t$ -SNE was derived. However, when the signal increases (lower left panel), our new method performs even better than  $t$ -SNE. In the scale difference scenario, Specc shows surprisingly high power. It performs

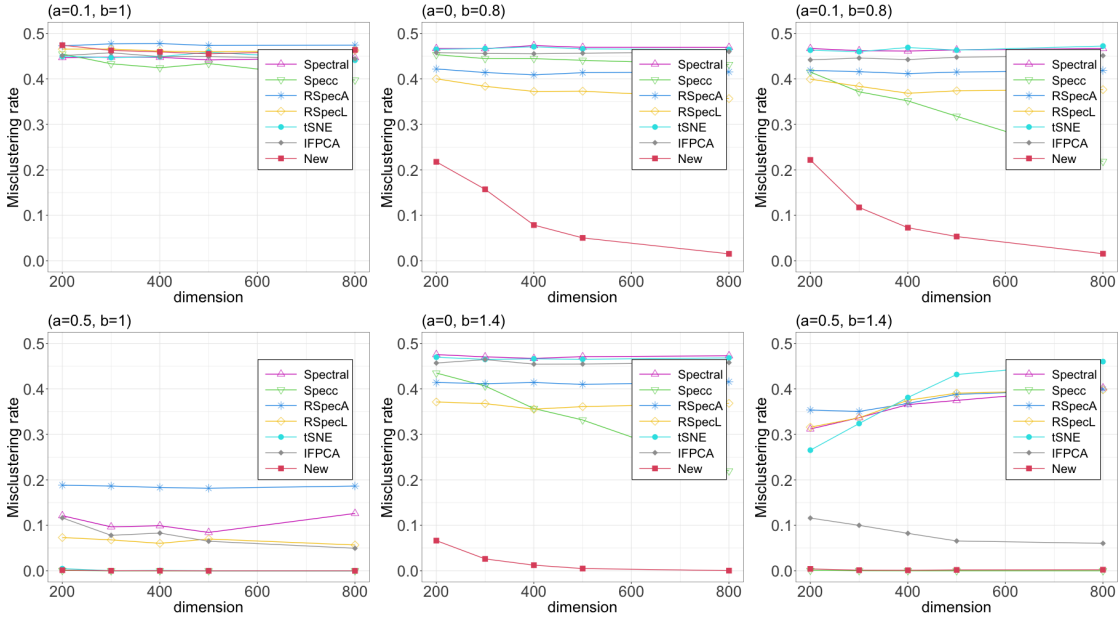


Fig. 7: Mis-clustering rates for Gaussian mixtures  $\mathcal{N}_d(\mathbf{0}, \Sigma)$  and  $\mathcal{N}_d(a\mathbf{1}, b\Sigma)$ .

slightly better than our new method, while other methods completely lose power. However, for the location-scale mixture case with moderate to high dimensions, our new method remains the most effective, followed by Specc,  $t$ -SNE, Spectral, and other methods.

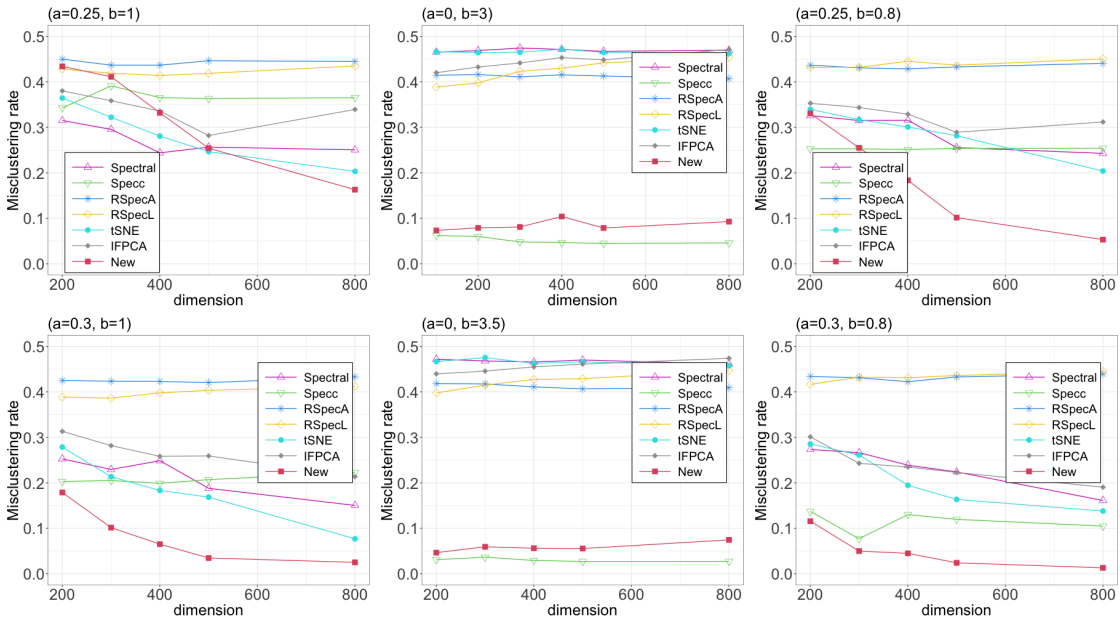


Fig. 8: Mis-clustering rates for multivariate  $t$ -distribution mixtures  $t_{20}(\mathbf{0}, \Sigma)$  and  $t_{20}(a\mathbf{1}, b\Sigma)$ .

To sum up, for the  $t_{20}$  distribution, our method remains the overall best among as the dimension  $d$  increases, with Specc slightly outperforming it in the scale difference scenario. While  $t$ -SNE performs significantly better compared to the Gaussian case, this is entirely expected because it was developed for heavy distribution distributions. All other methods are not as powerful as our new method in the  $t_{20}$  setting.

#### 4. REAL-WORLD APPLICATIONS

Here, we apply the proposed method to seven gene expression datasets, each with two classes and more features than the sample size: Alon et al. (1999); Golub et al. (1999); Wang et al. (2005); Gordon et al. (2002); Bhattacharjee et al. (2001); Singh et al. (2002); Su et al. (2001). The datasets are summarized in Table 3. Datasets 1, 2, and 6 were analyzed in Dettling (2004), while datasets 3, 5, and 7 were analyzed and grouped into two classes in Yousefi et al. (2010). Dataset 4 is from Gordon et al. (2002).

We summarize the datasets used in our analysis in Table 3. In all these datasets, the true labels are provided and are considered as the “ground truth”. These labels are only used to evaluate the error rate of various clustering methods. Table 4 displays the mis-clustering rates of different methods on these seven datasets.

For the Colon Cancer dataset, our new method achieves a mis-clustering rate of 0.112, while all other methods have a mis-clustering rate above 0.2. In a recent study (Singh & Verma, 2022), the best performance of various methods on the Colon Cancer dataset in terms of the Random Index (RI) was 51.77%. In comparison, our clustering result has an RI value of 79.64%, which is a significant improvement. It is noteworthy that the Colon Cancer dataset is known to be challenging for clustering, even for classification tasks where the labels of the training samples are available (Donoho & Jin, 2008). Therefore, achieving an 11.2% mis-clustering error is a breakthrough for the new method.

For the Leukemia dataset, all methods appear to be effective. Our method and Specc have the lowest mis-clustering rate at 4.2%. For the Lung Cancer (1) dataset, IF-PCA performs best with a mis-clustering rate of 3.3%. Our new method and Specc have a mis-clustering rate around 10%. Traditional Spectral clustering achieves a 5.5% misclustering rate. Other methods are not effective. For the Lung Cancer (2) dataset, several methods, including Specc, IF-PCA and our new methods, achieve equivalent best performance.

For the Breast Cancer, SuCancer, and Prostate Cancer datasets, none of the methods achieve a mis-clustering rate lower than 30%. New methods are needed for these three datasets. It is worth

Table 3: Dataset information

Data name	Abbreviation	Source	$n$	$p$
Colon Cancer	Cln	Alon et al. (99)	62	2000
Leukemia	Leuk	Golub et al. (99)	72	3571
Lung Cancer(1)	Lung1	Gordon et al. (02)	181	12,533
Lung Cancer(2)	Lung2	Bhattacharjee et al. (01)	203	12,600
Breast Cancer	Brst	Wang et al. (05)	276	22,215
Prostate Cancer	Prst	Singh et al. (02)	102	6033
SuCancer	Sur	Su et al. (01)	174	7909

Table 4: Mis-clustering rates on seven gene expression datasets.

Data	Spectral	Specc	RSpec(A)	RSpec(L)	IF-PCA	$t$ -SNE	New
Cln	0.467	0.451	0.209	0.258	0.403	0.415	<b>0.112</b>
Leuk	0.166	<b>0.042</b>	0.152	0.069	0.069	0.074	<b>0.042</b>
Lung1	0.055	0.093	0.254	0.403	<b>0.033</b>	0.466	0.116
Lung2	0.246	<b>0.217</b>	0.467	0.231	<b>0.217</b>	0.293	<b>0.217</b>
Brst	0.467	0.431	0.355	<b>0.344</b>	0.406	0.438	0.409
Sur	0.390	<b>0.333</b>	0.385	0.379	0.500	0.405	0.494
Prst	0.431	0.421	0.470	0.441	<b>0.382</b>	0.441	0.431

noting that the mis-clustering rate we report for IF-PCA on the SuCancer dataset differs from the number in [Jin & Wang \(2016\)](#) because we apply IF-PCA to the dataset without data modification.

In summary, the Breast Cancer, SuCancer, and Prostate Cancer datasets are extremely challenging for the existing methods. One possible reason might be that the two clusters in these datasets are not homogeneous. Aside from these extremely challenging datasets, our new method performs well for the remaining datasets and makes significant advancements for the Colon Cancer dataset.

## 5. CONCLUSION AND DISCUSSION

We proposed a new clustering framework that takes into account a useful pattern manifested by the curse of dimensionality in the  $k$ -NN graph, improving upon existing methods for clustering high-dimensional data, especially when there are two Gaussian clusters differ in scale. Two important parameters in our method are  $k$  in the  $k$ -NN graph and  $\kappa$  in  $M_\kappa = \max\{Z_w, \kappa Z_d\}$ . In this study, we focused on the traditional clustering task, which is an unsupervised learning task, and suggested using  $\kappa = 1.55$  and the value of  $k$  that results in the largest value of  $M_\kappa$ . In semi-supervised clustering, where we have partial labels of the data as well as a larger set of unlabeled data, the labeled data can be used to train the parameters  $k$  and  $\kappa$ .

In this study, we focused on two clusters, but many real-world datasets contain more than two clusters. When the number of clusters is fixed and known, we can use top-down divisive algorithms to extend this framework to multiple clusters. This involves recursively dividing a larger cluster into two smaller clusters until we reach the desired number of clusters. At each division step, a criterion such as the maximum value of  $M_\kappa$  can be used to determine which cluster to divide. Further research is needed to evaluate the performance of different criteria in this setting. When the number of clusters is unknown, the task becomes more challenging. In this case, a new penalized criterion that combines  $M_\kappa$  and BIC may be considered, but extensive investigation is required.

## ACKNOWLEDGEMENT

Hao Chen and Xiancheng Lin were supported in part by the NSF awards DMS-1848579 and DMS-2311399.

## REFERENCES

ALON, U., BARKAI, N., NOTTERMAN, D. A., GISH, K., YBARRA, S., MACK, D. & LEVINE, A. J. (1999). Broad patterns of gene expression revealed by clustering analysis of tumor and normal colon tissues probed by oligonucleotide

- arrays. *Proceedings of the National Academy of Sciences* **96**, 6745–6750.
- BAJWA, M. S., AGARWAL, A. P. & MANCHANDA, S. (2015). Ternary search algorithm: Improvement of binary search. In *2015 2nd International Conference on Computing for Sustainable Global Development (INDIACom)*. IEEE.
- BHATTACHARJEE, A., RICHARDS, W. G., STAUNTON, J., LI, C., MONTI, S., VASA, P., LADD, C., BEHESHTI, J., BUENO, R., GILLETTE, M. et al. (2001). Classification of human lung carcinomas by mrna expression profiling reveals distinct adenocarcinoma subclasses. *Proceedings of the National Academy of Sciences* **98**, 13790–13795.
- CHAN, P. K., SCHLAG, M. D. & ZIEN, J. Y. (1993). Spectral k-way ratio-cut partitioning and clustering. In *Proceedings of the 30th international Design Automation Conference*.
- CHEN, H. & FRIEDMAN, J. H. (2017). A new graph-based two-sample test for multivariate and object data. *Journal of the American statistical association* **112**, 397–409.
- DETLING, M. (2004). Bagboosting for tumor classification with gene expression data. *Bioinformatics* **20**, 3583–3593.
- DONOHO, D. & JIN, J. (2008). Higher criticism thresholding: Optimal feature selection when useful features are rare and weak. *Proceedings of the National Academy of Sciences* **105**, 14790–14795.
- GOLUB, T. R., SLONIM, D. K., TAMAYO, P., HUARD, C., GAASENBEEK, M., MESIROV, J. P., COLLER, H., LOH, M. L., DOWNING, J. R., CALIGIURI, M. A. et al. (1999). Molecular classification of cancer: class discovery and class prediction by gene expression monitoring. *science* **286**, 531–537.
- GORDON, G. J., JENSEN, R. V., HSIAO, L.-L., GULLANS, S. R., BLUMENSTOCK, J. E., RAMASWAMY, S., RICHARDS, W. G., SUGARBAKER, D. J. & BUENO, R. (2002). Translation of microarray data into clinically relevant cancer diagnostic tests using gene expression ratios in lung cancer and mesothelioma. *Cancer research* **62**, 4963–4967.
- HASTIE, T., TIBSHIRANI, R., FRIEDMAN, J. H. & FRIEDMAN, J. H. (2009). *The elements of statistical learning: data mining, inference, and prediction*, vol. 2. Springer.
- HENZE, N. (1988). A multivariate two-sample test based on the number of nearest neighbor type coincidences. *The Annals of Statistics* **16**, 772–783.
- JIN, J. & WANG, W. (2016). Influential features pca for high dimensional clustering. *The Annals of Statistics* **44**, 2323–2359.
- LEIGHTON, F. T. & RAO, S. (1988). An approximate max-flow min-cut theorem for uniform multicommodity flow problems with applications to approximation algorithms. In *FOCS*, vol. 88.
- LIU, Y.-W. & CHEN, H. (2022). A fast and efficient change-point detection framework based on approximate  $k$ -nearest neighbor graphs. *IEEE Transactions on Signal Processing* **70**, 1976–1986.
- MAATEN, L. v. d. & HINTON, G. (2008). Visualizing data using t-sne. *Journal of Machine Learning Research* **9**, 2579–2605.
- MWANGI, B., SOARES, J. C. & HASAN, K. M. (2014). Visualization and unsupervised predictive clustering of high-dimensional multimodal neuroimaging data. *Journal of neuroscience methods* **236**, 19–25.
- ROHE, K., CHATTERJEE, S. & YU, B. (2011). Spectral clustering and the high-dimensional stochastic blockmodel .
- SCHILLING, M. F. (1986). Multivariate two-sample tests based on nearest neighbors. *Journal of the American Statistical Association* **81**, 799–806.
- SHI, J. & MALIK, J. (2000). Normalized cuts and image segmentation. *IEEE Transactions on pattern analysis and machine intelligence* **22**, 888–905.
- SINGH, D., FEBBO, P. G., ROSS, K., JACKSON, D. G., MANOLA, J., LADD, C., TAMAYO, P., RENSHAW, A. A., D’AMICO, A. V., RICHIE, J. P. et al. (2002). Gene expression correlates of clinical prostate cancer behavior. *Cancer cell* **1**, 203–209.
- SINGH, V. & VERMA, N. K. (2022). Gene expression data analysis using feature weighted robust fuzzy-means clustering. *IEEE Transactions on NanoBioscience* **22**, 99–105.
- SU, A. I., WELSH, J. B., SAPINOSO, L. M., KERN, S. G., DIMITROV, P., LAPP, H., SCHULTZ, P. G., POWELL, S. M., MOSKALUK, C. A., FRIERSON JR, H. F. et al. (2001). Molecular classification of human carcinomas by use of gene expression signatures. *Cancer research* **61**, 7388–7393.
- VON LUXBURG, U. (2007). A tutorial on spectral clustering. *Statistics and computing* **17**, 395–416.
- WANG, Y., KLJUN, J. G., ZHANG, Y., SIEUWERTS, A. M., LOOK, M. P., YANG, F., TALANTOV, D., TIMMERMANS, M., MEIJER-VAN GELDER, M. E., YU, J. et al. (2005). Gene-expression profiles to predict distant metastasis of lymph-node-negative primary breast cancer. *The Lancet* **365**, 671–679.
- WU, Z. & LEAHY, R. (1993). An optimal graph theoretic approach to data clustering: Theory and its application to image segmentation. *IEEE transactions on pattern analysis and machine intelligence* **15**, 1101–1113.
- YOUSEFI, M. R., HUA, J., SIMA, C. & DOUGHERTY, E. R. (2010). Reporting bias when using real data sets to analyze classification performance. *Bioinformatics* **26**, 68–76.
- ZHANG, Y. & CHEN, H. (2021). Graph-based multiple change-point detection. *arXiv preprint arXiv:2110.01170* .
- ZHOU, D. & CHEN, H. (2022). Ring-cpd: Asymptotic distribution-free change-point detection for multivariate and non-euclidean data. *arXiv preprint arXiv:2206.03038* .
- ZHU, Y. & CHEN, H. (2021). Limiting distributions of graph-based test statistics. *arXiv preprint arXiv:2108.07446* .